

Coupled effects of electrical polarization-strain gradient on vibration behavior of double-layered flexoelectric nanoplates

Mohammad Reza Barati*

Aerospace Engineering Department & Center of Excellence in Computational Aerospace,
Amirkabir University of Technology, Tehran, Iran

(Received June 23, 2017, Revised July 30, 2017, Accepted September 5, 2017)

Abstract. A vibrating double-layered nanoscale piezoelectric plate is developed accounting for the flexoelectricity and surface effects. The flexoelectricity is due to the coupling between electrical polarization and strain gradient. Applying Hamilton's principle, the governing equations and related boundary conditions are derived. Assuming suitable approximate functions, the governing equations are numerically solved for simply-supported and clamped boundary conditions. Obtained results indicate that both the flexoelectricity and surface effects possess notable impact on the vibration frequencies of the system. Only flexoelectricity yields a considerable difference between the present model and previous investigations on conventional piezoelectric nanoplates. Generally, a parametric study has been performed to examine the effects of surface elasticity, flexoelectricity, applied electric voltage, interlayer stiffness, geometrical parameters and boundary conditions on vibration frequencies of piezoelectric nanoplates.

Keywords: vibration; flexoelectric nanoplate; surface effect; double-layered nanoplate

1. Introduction

Nowadays, nanoscale piezoelectric structures have gained many interests in scientific communities due to their potential applications as sensors and energy harvesters in the nanoelectromechanical systems (NEMS) because of possessing excellent electromechanical coupling and unique specifications at the submicron scale (Ebrahimi and Barati 2017). Thus, it is of great importance to obtain a comprehensive understanding on the electromechanical coupling behaviors of a piezoelectric structure at the nanoscale.

Recently, molecular dynamics simulations and experimental observations have indicated that the elastic and piezoelectric constants of a piezoelectric material become size-dependent at the nanoscale (Zhang *et al.* 2009). Such an important fact distinguishes a nanoscale piezoelectric material from a macroscopic bulk counterpart. Accordingly, many investigations have been performed to understand the size-dependent mechanical behaviors of piezoelectric nanostructures by means of higher order elasticity theories which are capable of describing the size effects. A linear surface elasticity theory (Gurtin and Murdoch 1975) is introduced to incorporate the size-dependent properties of nanomaterials with surface effects raised from the large ratio of surface area to volume. This theory introduces surface layers having zero thickness with specified elastic constants attached to a bulk material. Based on this theory, the size-dependent static and dynamic

characteristics of piezoelectric nanostructures have been widely investigated (Asemi *et al.* 2014, Zang *et al.* 2014, Zhang *et al.* 2014, Arani *et al.* 2015, Li and Pan 2016, Wang *et al.* 2016, Yan 2016, Shen *et al.* 2017, Karimi and Shahidi 2017). Recently, size-dependent analysis of nanostructures by means of nonlocal elastic field theory of Eringen (1983) has received wide importance. Nonlocal elasticity theory has the potential to describe the long range interactions between atoms inside the material. The prominence of nonlocal elasticity has stimulated the researchers for modeling and analysis of the nanoscale structures (Barati and Shahverdi 2017, Gholami and Ansari 2017, Elmerabet *et al.* 2017, Ebrahimi and Salari 2017, Li and Hu 2016, Akbas 2016, Li *et al.* 2016, Abouel *et al.* 2016, Bounouara *et al.* 2016, Ebrahimi and Barati 2016, Asemi *et al.* 2014).

The flexoelectricity is known as a specific electromechanical coupling phenomenon between electrical polarization and strain gradients. It is reported that the strain gradients or non-uniform strain fields can locally break the inversion symmetry of the materials and thus induce the polarization in the structures. Such important phenomenon has been neglected in above-mentioned studies on piezoelectric nanostructures. Actually, the flexoelectricity provides an inherent size effect in small scale structures which is not available in the additional piezoelectricity. Recently, this important phenomenon is considered in some investigations on piezoelectric nanostructures. Surface and flexoelectricity effects on static response of piezoelectric nanobeams are examined by Liang *et al.* (2014). Static behavior of a piezoelectric nanobeam with integrated flexoelectric layers acting as nanoactuators is analyzed by Ray (2016). A size-dependent bending and vibration analysis of flexoelectric nanobeams is presented by Yan and Jiang (2013) based on Timoshenko beam theory. Surface

*Corresponding author, Assistant Professor
E-mail: mrb.barati@ymail.com

and flexoelectricity effects on static response of piezoelectric nanoplates under uniform static load are examined by Zhang and Jiang (2014). They showed that configuration of a piezoelectric nanoplate in bending is significantly affected by the flexoelectricity and applied voltage. Ebrahimi and Barati (2017b,c) examined surface effects on linear vibration behavior of open circuit flexoelectric nanobeams and nanoplates. Liang *et al.* (2016) examined buckling and vibration responses of open circuit flexoelectric nanofilms subjected to mechanical loads. One can see that analysis of flexoelectric nanostructures is still at the beginning stage. In fact, literature survey indicates that there is no published paper on vibration analysis of double-layered or elastically connected flexoelectric nanoplates under closed circuit electric field condition.

In the present analysis, a size-dependent vibrating model of a double-layered flexoelectric nanoplate is proposed based on the classical plate model and the flexoelectricity theory with consideration of surface effects. For the first time, out-of-phase and in-phase vibrations of a double-layered flexoelectric nanoplate system are reported. The governing equations and boundary conditions of a double-layered flexoelectric nanoplate under closed circuit conditions are derived from Hamilton's principle. To illustrate the newly developed flexoelectric plate model, the free vibration problem of a simply supported and clamped plates is solved, and the corresponding numerical results are analyzed to show the importance of flexoelectric coefficient, surface elasticity, interlayer stiffness, applied voltage and nanoplate thickness on vibration frequencies. Obtained results can serve as a useful guidance for better modeling and analysis of double-layered piezoelectric nanostructures.

2. Modeling of piezoelectric nanoplate with surface and flexoelectric effects

Surface effects have been taken into consideration by assuming that the nanoplate is divided to a bulk part as well as surface layers having ignorable thickness as indicated in Fig. 1. Also, different models of vibration of system is shown in Fig. 2. As stated, the flexoelectricity influence is incorporated into the surface piezoelectricity theory by the strain gradient-polarization and also the polarization gradient-strain couplings. The bulk energy density can be represented by (Yang *et al.* 2015)

$$U_b = \frac{1}{2} a_{kl} P_k P_l + \frac{1}{2} c_{ijkl} \varepsilon_{ij} \varepsilon_{kl} + d_{ijk} P_k \varepsilon_{ij} + \frac{1}{2} b_{ijkl} P_{i,j} P_{k,l} + f_{ijkl} u_{i,jk} P_l + e_{ijm} \varepsilon_{ij} P_{k,l} \quad (1)$$

Here, P_i and ε_{ij} are the polarization and strain tensors, respectively; c_{ijkl} , a_{kl} and d_{ijk} denote the elastic, reciprocal dielectric susceptibility and piezoelectric material constants, respectively. Also, b_{ijkl} represent the coupling between polarization gradients. Finally, f_{ijkl} is the flexoelectricity coefficient representing the coupling of strain gradient and polarization.

Finally, the constitutive relations for the bulk considering flexoelectricity effects can be written as (Yang

et al. 2015)

$$\sigma_{ij} = \frac{\partial U_b}{\partial \varepsilon_{ij}} = C_{ijkl} \varepsilon_{kl} + d_{ijk} P_k + e_{ijkl} \frac{\partial P_k}{\partial x_l} \quad (2a)$$

$$\sigma_{ijm} = \frac{\partial U_b}{\partial \varepsilon_{ij} / \partial x_m} = f_{ijmk} P_k \quad (2b)$$

$$E_i = \frac{\partial U_b}{\partial P_i} = a_{ij} P_j + d_{jki} \varepsilon_{jk} + f_{jkli} u_{j,kl} \quad (2c)$$

$$E_{ij} = \frac{\partial U_b}{\partial P_i / \partial x_j} = b_{ijkl} P_{k,l} + e_{klij} \varepsilon_{kl} \quad (2d)$$

where σ_{ij} and E_i denote the stress and electric field tensors, respectively.

To consider the surface effects, i.e., the residual surface stress, the surface elasticity, and the surface piezoelectricity, the surface internal energy density U_s can be defined as

$$U_s = U_{s0} + \Gamma_{\alpha\beta} \varepsilon_{\alpha\beta}^s + \frac{1}{2} a_{\alpha\beta}^s P_\alpha^s P_\beta^s + \frac{1}{2} c_{\alpha\beta\gamma\kappa}^s \varepsilon_{\alpha\beta}^s \varepsilon_{\gamma\kappa}^s + d_{\alpha\beta\gamma}^s P_\gamma^s \varepsilon_{\alpha\beta}^s \quad (3)$$

where P_α^s and $\varepsilon_{\alpha\beta}^s$ are surface polarization and surface strain tensors, respectively. Also, $\Gamma_{\alpha\beta} = \sigma_0 \delta_{\alpha\beta}$ is surface residual stress tensor; $a_{\alpha\beta}^s$ and $c_{\alpha\beta\gamma\kappa}^s$ denote the surface dielectric susceptibility and surface elastic constants. Also, the surface piezoelectric constants are represented by $d_{\alpha\beta\gamma}^s$. Thus, the surface constitutive relations can be expressed by

$$\sigma_{\alpha\beta}^s = \frac{\partial U_s}{\partial \varepsilon_{\alpha\beta}^s} = \Gamma_{\alpha\beta} + c_{\alpha\beta\gamma\kappa}^s \varepsilon_{\gamma\kappa}^s + d_{\alpha\beta\gamma}^s P_\gamma^s \quad (4a)$$

$$E_\alpha^s = \frac{\partial U_s}{\partial P_\alpha^s} = a_{\alpha\beta}^s P_\beta^s + d_{\beta\alpha\gamma}^s \varepsilon_{\beta\gamma}^s \quad (4b)$$

in which $\sigma_{\alpha\beta}^s$ and E_α^s are the surface stress tensor and surface electric field vector.

3. Theoretical formulation

In this study, the classical plate theory is adopted for modeling of a thin flexoelectric nanoplate accounting for surface effects. Thus, it is possible to represent the displacement field of the nanoplate as

$$u_1(x, y, z) = u(x, y) - z \frac{\partial w(x, y)}{\partial x} \quad (5a)$$

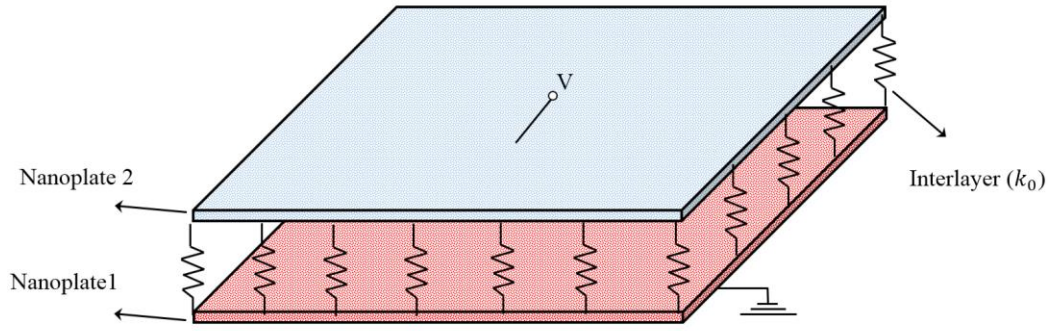


Fig. 1 Geometry and coordinates of flexoelectric nanoplate system

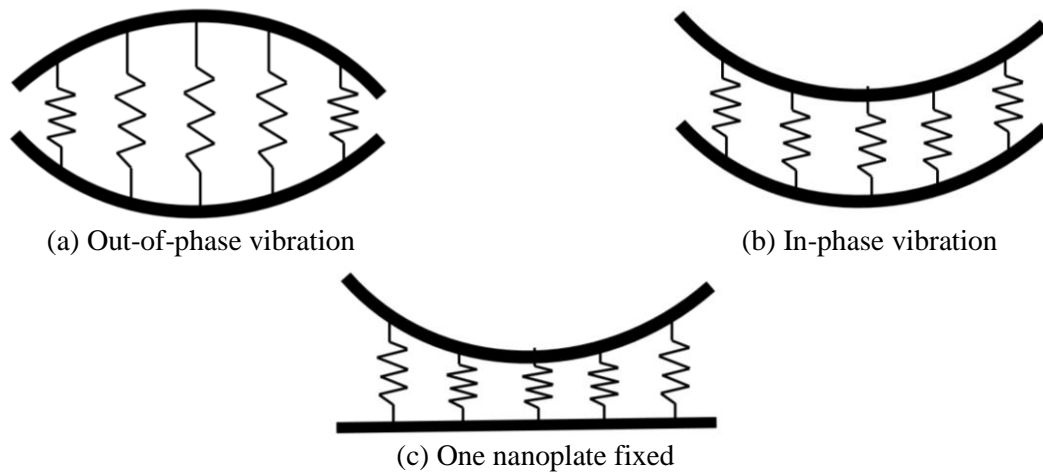


Fig. 2 Different types of motion for a double-layered nanoplate

$$u_2(x, y, z) = v(x, y) - z \frac{\partial w(x, y)}{\partial y} \quad (5b)$$

$$u_3(x, y, z) = w(x, y) \quad (5c)$$

where u and v are in-plane displacements, respectively and w is the lateral displacement. Then, the strains and strain-gradients are obtained as

$$\begin{aligned} \varepsilon_{xx} &= \frac{\partial u_1}{\partial x} = \frac{\partial u}{\partial x} - z \frac{\partial^2 w}{\partial x^2}, & \varepsilon_{yy} &= \frac{\partial u_2}{\partial y} = \frac{\partial v}{\partial y} - z \frac{\partial^2 w}{\partial y^2} \\ \gamma_{xy} &= \frac{\partial u_1}{\partial y} + \frac{\partial u_2}{\partial x} = \frac{\partial u}{\partial y} + \frac{\partial v}{\partial x} - 2z \frac{\partial^2 w}{\partial x \partial y} \\ \eta_{xxz} &= \frac{\partial \varepsilon_{xx}}{\partial z} = -\frac{\partial^2 w}{\partial x^2}, & \eta_{yyz} &= \frac{\partial \varepsilon_{yy}}{\partial z} = -\frac{\partial^2 w}{\partial y^2} \\ \eta_{xyz} &= \frac{\partial \gamma_{xy}}{\partial z} = -2 \frac{\partial^2 w}{\partial x \partial y} \end{aligned} \quad (6)$$

The polarization direction is assumed as the same as z -direction or transverse direction. Thus, the electric field in this direction is defined as

$$E_z = -\frac{\partial \Phi}{\partial z} \quad (7)$$

where Φ is the electrostatic potential. Inserting Eq. (6) into Eq. (2(e)) gives

$$E_z = a_{33} P_z + d_{31} \left(\frac{\partial u}{\partial x} + \frac{\partial v}{\partial y} - z \frac{\partial^2 w}{\partial x^2} - z \frac{\partial^2 w}{\partial y^2} \right) - f_{31} \left(\frac{\partial^2 w}{\partial x^2} + \frac{\partial^2 w}{\partial y^2} \right) \quad (8)$$

The Gauss's law requires the following relation in absence of the free electric charges

$$-\kappa \Phi_{,zz} + P_{z,z} = 0 \quad (9)$$

in which $\kappa = \kappa_0 \kappa_b$. Here, $\kappa_0 = 8.85 \times 10^{-12} \text{ CV}^{-1} \text{ m}^{-1}$ and $\kappa_b = 6.62$ are the permittivity of the air and the background permittivity. Also, electric boundary conditions under closed circuit conditions are

$$\Phi\left(\frac{h}{2}\right) = V, \quad \Phi\left(-\frac{h}{2}\right) = 0 \quad (10)$$

Now, substituting Eqs. (8) and (10) into Eq. (9) gives the following expressions electric potential, electric field and

electrical polarization as

$$\Phi = \frac{d_{31}}{2(1+a_{33}\kappa)} \left(\frac{\partial^2 w}{\partial x^2} + \frac{\partial^2 w}{\partial y^2} \right) \left(z^2 - \frac{1}{4}h^2 \right) + \frac{V}{h}z + \frac{V}{2} + \frac{f_{31}}{(1+a_{33}\kappa)} \left(\frac{\partial^2 w}{\partial x^2} + \frac{\partial^2 w}{\partial y^2} \right) z - \frac{f_{31}h}{2(1+a_{33}\kappa)} \left(\frac{\partial^2 w}{\partial x^2} + \frac{\partial^2 w}{\partial y^2} \right) \frac{e^{\lambda z} - e^{-\lambda z}}{e^{\frac{h}{2}\lambda} - e^{-\frac{h}{2}\lambda}} \quad (11a)$$

$$E_z = -\frac{d_{31}}{(1+a_{33}\kappa)} \left(\frac{\partial^2 w}{\partial x^2} + \frac{\partial^2 w}{\partial y^2} \right) z - \frac{V}{h} + \frac{a_{33}\kappa f_{31}}{(1+a_{33}\kappa)} \left(\frac{\partial^2 w}{\partial x^2} + \frac{\partial^2 w}{\partial y^2} \right) - \frac{a_{33}f_{31}h}{2\lambda b_{33}} \left(\frac{\partial^2 w}{\partial x^2} + \frac{\partial^2 w}{\partial y^2} \right) \frac{e^{\lambda z} + e^{-\lambda z}}{e^{\frac{h}{2}\lambda} - e^{-\frac{h}{2}\lambda}} \quad (11b)$$

$$P_z = \frac{d_{31}\kappa}{(1+a_{33}\kappa)} \left(\frac{\partial^2 w}{\partial x^2} + \frac{\partial^2 w}{\partial y^2} \right) z - \frac{V}{a_{33}h} + \frac{f_{31}(1+2a_{33}\kappa)}{a_{33}(1+a_{33}\kappa)} \left(\frac{\partial^2 w}{\partial x^2} + \frac{\partial^2 w}{\partial y^2} \right) - \frac{f_{31}h}{2\lambda b_{33}} \left(\frac{\partial^2 w}{\partial x^2} + \frac{\partial^2 w}{\partial y^2} \right) \frac{e^{\lambda z} + e^{-\lambda z}}{e^{\frac{h}{2}\lambda} - e^{-\frac{h}{2}\lambda}} \quad (11c)$$

in which $\lambda = \sqrt{\frac{1+a_{33}\kappa}{b_{33}\kappa}}$. It is now possible to obtain stress field using Eq. (2) as

$$\sigma_{xx} = \left(-c_{11} + \frac{d_{31}^2\kappa}{1+a_{33}\kappa} \right) z \frac{\partial^2 w}{\partial x^2} + \left(-c_{12} + \frac{d_{31}^2\kappa}{1+a_{33}\kappa} \right) z \frac{\partial^2 w}{\partial y^2} - \frac{d_{31}V}{a_{33}h} + \left(\frac{d_{31}f_{31}}{a_{33}} - \frac{d_{31}f_{31}h}{2\lambda b_{33}} \frac{e^{\lambda z} + e^{-\lambda z}}{e^{\frac{h}{2}\lambda} - e^{-\frac{h}{2}\lambda}} + \frac{f_{31}^2h}{2b_{33}} \frac{e^{\lambda z} - e^{-\lambda z}}{e^{\frac{h}{2}\lambda} - e^{-\frac{h}{2}\lambda}} \right) \left(\frac{\partial^2 w}{\partial x^2} + \frac{\partial^2 w}{\partial y^2} \right) \quad (12)$$

$$\sigma_{yy} = \left(-c_{12} + \frac{d_{31}^2\kappa}{1+a_{33}\kappa} \right) z \frac{\partial^2 w}{\partial x^2} + \left(-c_{11} + \frac{d_{31}^2\kappa}{1+a_{33}\kappa} \right) z \frac{\partial^2 w}{\partial y^2} - \frac{d_{31}V}{a_{33}h} + \left(\frac{d_{31}f_{31}}{a_{33}} - \frac{d_{31}f_{31}h}{2\lambda b_{33}} \frac{e^{\lambda z} + e^{-\lambda z}}{e^{\frac{h}{2}\lambda} - e^{-\frac{h}{2}\lambda}} + \frac{f_{31}^2h}{2b_{33}} \frac{e^{\lambda z} - e^{-\lambda z}}{e^{\frac{h}{2}\lambda} - e^{-\frac{h}{2}\lambda}} \right) \left(\frac{\partial^2 w}{\partial x^2} + \frac{\partial^2 w}{\partial y^2} \right) \quad (13)$$

$$\sigma_{xy} = -2c_{66}z \frac{\partial^2 w}{\partial x \partial y} \quad (14)$$

Moreover, the surface stresses of a flexoelectric nanoplate under electric loading can be expressed by

$$\sigma_{xx}^s = \sigma_0 + \left(-c_{11}^s + \frac{d_{31}^s d_{31}^s \kappa}{1+a_{33}\kappa} \right) z \frac{\partial^2 w}{\partial x^2} + \left(-c_{12}^s + \frac{d_{31}^s d_{31}^s \kappa}{1+a_{33}\kappa} \right) z \frac{\partial^2 w}{\partial y^2} - \frac{d_{31}^s V}{a_{33}h} + \left(\frac{d_{31}^s f_{31} (1+2a_{33}\kappa)}{a_{33}(1+a_{33}\kappa)} - \frac{d_{31}^s f_{31} h}{2\lambda b_{33}} \frac{e^{\lambda z} + e^{-\lambda z}}{e^{\frac{h}{2}\lambda} - e^{-\frac{h}{2}\lambda}} \right) \left(\frac{\partial^2 w}{\partial x^2} + \frac{\partial^2 w}{\partial y^2} \right) \quad (15)$$

$$\sigma_{yy}^s = \sigma_0 + \left(-c_{12}^s + \frac{d_{31}^s d_{31}^s \kappa}{1+a_{33}\kappa} \right) z \frac{\partial^2 w}{\partial x^2} + \left(-c_{11}^s + \frac{d_{31}^s d_{31}^s \kappa}{1+a_{33}\kappa} \right) z \frac{\partial^2 w}{\partial y^2} - \frac{d_{31}^s V}{a_{33}h} + \left(\frac{d_{31}^s f_{31} (1+2a_{33}\kappa)}{a_{33}(1+a_{33}\kappa)} - \frac{d_{31}^s f_{31} h}{2\lambda b_{33}} \frac{e^{\lambda z} + e^{-\lambda z}}{e^{\frac{h}{2}\lambda} - e^{-\frac{h}{2}\lambda}} \right) \left(\frac{\partial^2 w}{\partial x^2} + \frac{\partial^2 w}{\partial y^2} \right) \quad (16)$$

$$\sigma_{xy}^s = -2c_{66}^s z \frac{\partial^2 w}{\partial x \partial y} \quad (17)$$

Through extended Hamilton's principle, the governing equations can be derived as follows

$$\delta \int_{t_1}^{t_2} \left(-\int_{\Omega} H d\Omega + K + W \right) = 0 \quad (18)$$

in which K and W are kinetic energy and work done by non-conservative forces. Also, $H=H_b+H_s$ is the electric enthalpy including both the bulk and surface components.

$$H_b = U_b - \frac{1}{2} \kappa \Phi_i \Phi_j + \Phi_i P_i \quad (19)$$

$$H_s = U_s + \Phi_k^s P_k^s \quad (20)$$

where Φ^s is surface electric potential. Inserting Eqs. (1) and (3) into Eqs. (19) and (20) yields

$$H = \frac{1}{2} \left(\sigma_{xx} \varepsilon_{xx} + \sigma_{yy} \varepsilon_{yy} + \sigma_{xy} \gamma_{xy} + \sigma_{xz} \eta_{xz} + \sigma_{yz} \eta_{yz} + \sigma_{xyz} \eta_{xyz} \right) + \frac{1}{2} \left(\sigma_{xx}^s \delta \varepsilon_{xx} + \sigma_{yy}^s \delta \varepsilon_{yy} + \sigma_{xy}^s \delta \gamma_{xy} \right) + U_{s0} - \frac{1}{2} \kappa \Phi_z \Phi_z + \Phi_z P_z \quad (21)$$

while internal energy variation using Eqs. (1) and (3) can be expressed as

$$\delta U = \int_0^h \int_0^h \left((N_{xx} + N_{xx}^s) \frac{\partial \delta u}{\partial x} - (M_{xx} + M_{xx}^s) \frac{\partial^2 \delta w}{\partial x^2} + (N_{yy} + N_{yy}^s) \frac{\partial \delta v}{\partial y} - (M_{yy} + M_{yy}^s) \frac{\partial^2 \delta w}{\partial y^2} + (N_{xy} + N_{xy}^s) \left(\frac{\partial \delta u}{\partial y} + \frac{\partial \delta v}{\partial x} \right) - 2(M_{xy} + M_{xy}^s) \frac{\partial^2 \delta w}{\partial x \partial y} + P_{xx} \frac{\partial^2 \delta w}{\partial x^2} + P_{yy} \frac{\partial^2 \delta w}{\partial y^2} + P_{xyz} \frac{\partial^2 \delta w}{\partial y^2} \right) dx dy \quad (22)$$

in which

$$(N_i, M_i) = \int_A (1, z) \sigma_i dA, \quad i = (x, y, xy) \quad (23)$$

$$P_i = \int_A \tau_i dA, \quad i = (xxz, yyz)$$

The work done by applied forces can be written in the form

$$\delta W = \int_0^a \int_0^b \left(N_x^0 \frac{\partial w}{\partial x} \frac{\partial \delta w}{\partial x} + N_y^0 \frac{\partial w}{\partial y} \frac{\partial \delta w}{\partial y} \right) dx dy \quad (24)$$

where N_x^0, N_y^0 are in-plane applied loads. The first variational of the virtual kinetic energy of present plate model can be written in the form as

$$\delta K = \int_0^a \int_0^b \left[I_0 \left(\frac{\partial u}{\partial t} \frac{\partial \delta u}{\partial t} + \frac{\partial v}{\partial t} \frac{\partial \delta v}{\partial t} + \frac{\partial w}{\partial t} \frac{\partial \delta w}{\partial t} \right) - I_1 \left(\frac{\partial u}{\partial t} \frac{\partial \delta w}{\partial x \partial t} + \frac{\partial w}{\partial x \partial t} \frac{\partial \delta u}{\partial t} + \frac{\partial v}{\partial t} \frac{\partial \delta w}{\partial y \partial t} + \frac{\partial w}{\partial y \partial t} \frac{\partial \delta v}{\partial t} \right) + I_2 \left(\frac{\partial w}{\partial x \partial t} \frac{\partial \delta w}{\partial x \partial t} + \frac{\partial w}{\partial y \partial t} \frac{\partial \delta w}{\partial y \partial t} \right) \right] dx dy \quad (25)$$

in which the mass inertias are defined as

$$(I_0, I_1, I_2) = \int_{-h/2}^{h/2} (1, z, z^2) \rho dz \quad (26)$$

The following Euler-Lagrange equations are obtained by inserting Eqs. (21)-(25) in Eq. (18) when the coefficients of $\delta u, \delta v, \delta w$ are equal to zero

$$\frac{\partial(N_{xx} + N_{xx}^s)}{\partial x} + \frac{\partial(N_{xy} + N_{xy}^s)}{\partial y} = I_0 \frac{\partial^2 u}{\partial t^2} \quad (27a)$$

$$\frac{\partial(N_{xy} + N_{xy}^s)}{\partial x} + \frac{\partial(N_{yy} + N_{yy}^s)}{\partial y} = I_0 \frac{\partial^2 v}{\partial t^2} \quad (27b)$$

$$\frac{\partial^2(M_{xx} + M_{xx}^s)}{\partial x^2} + 2 \frac{\partial^2(M_{xy} + M_{xy}^s)}{\partial x \partial y} + \frac{\partial^2(M_{yy} + M_{yy}^s)}{\partial y^2} + \frac{\partial^2 P_{xxz}}{\partial x^2} + \frac{\partial^2 P_{yyz}}{\partial y^2} - 2\sigma_0 \nabla^2 w = I_0 \frac{\partial^2 w}{\partial t^2} - I_2 \nabla^2 \left(\frac{\partial^2 w}{\partial t^2} \right) \quad (27c)$$

and the associated boundary conditions

$$u = 0, \text{ or } (N_{xx} + N_{xx}^s)n_x + (N_{xy} + N_{xy}^s)n_y = 0 \quad (28a)$$

$$v = 0, \text{ or } (N_{xy} + N_{xy}^s)n_x + (N_{yy} + N_{yy}^s)n_y = 0 \quad (28b)$$

$$w = 0, \text{ or } n_x \left(\frac{\partial(M_{xx} + M_{xx}^s)}{\partial x} + \frac{\partial(M_{xy} + M_{xy}^s)}{\partial y} + \frac{\partial P_{xxz}}{\partial x} \right) + n_y \left(\frac{\partial(M_{xy} + M_{xy}^s)}{\partial y} + \frac{\partial(M_{yy} + M_{yy}^s)}{\partial x} + \frac{\partial P_{yyz}}{\partial y} \right) = 0 \quad (28c)$$

$$\frac{\partial w}{\partial x} = 0, \text{ or } (M_{xx} + M_{xx}^s)n_x + (M_{xy} + M_{xy}^s)n_y = 0 \quad (28d)$$

$$\frac{\partial w}{\partial y} = 0, \text{ or } (M_{xy} + M_{xy}^s)n_x + (M_{yy} + M_{yy}^s)n_y = 0 \quad (28e)$$

Finally, the governing equations of each nanoplate in terms of displacements can be obtained using Eqs. (12)-(14) and (27) as

$$D_{11} \left(\frac{\partial^4 w_1}{\partial x^4} + \frac{\partial^4 w_1}{\partial y^4} \right) + 2(D_{12} + 2D_{66}) \frac{\partial^4 w_1}{\partial x^2 \partial y^2} + \left(\frac{d_{31}}{a_{33}} V + \frac{2d_{31}^2}{a_{33} h} V - 2\sigma_0 \right) \left(\frac{\partial^2 w_1}{\partial x^2} + \frac{\partial^2 w_1}{\partial y^2} \right) - \rho \frac{h^3}{12} \left(\frac{\partial^2 \ddot{w}_1}{\partial x^2} + \frac{\partial^2 \ddot{w}_1}{\partial y^2} \right) + \rho h \ddot{w}_1 + k_0 (w_1 - w_2) = 0 \quad (29a)$$

$$D_{11} \left(\frac{\partial^4 w_2}{\partial x^4} + \frac{\partial^4 w_2}{\partial y^4} \right) + 2(D_{12} + 2D_{66}) \frac{\partial^4 w_2}{\partial x^2 \partial y^2} + \left(\frac{d_{31}}{a_{33}} V + \frac{2d_{31}^2}{a_{33} h} V - 2\sigma_0 \right) \left(\frac{\partial^2 w_2}{\partial x^2} + \frac{\partial^2 w_2}{\partial y^2} \right) - \rho \frac{h^3}{12} \left(\frac{\partial^2 \ddot{w}_2}{\partial x^2} + \frac{\partial^2 \ddot{w}_2}{\partial y^2} \right) + \rho h \ddot{w}_2 - k_0 (w_1 - w_2) = 0 \quad (29b)$$

in which

$$D_{11} = \left(c_{11} - \frac{d_{31}^2 \kappa}{1 + \kappa a_{33}} \right) \frac{h^3}{12} - \frac{f_{31}^2 h}{a_{33} (1 + \kappa a_{33})} - \frac{f_{31}^2 h^2}{2\lambda b_{33}} * \frac{e^{\frac{h}{2}\lambda} + e^{-\frac{h}{2}\lambda}}{e^{\frac{h}{2}\lambda} - e^{-\frac{h}{2}\lambda}} + \frac{b_{33} d_{31}^2 \kappa^2 h}{(1 + \kappa a_{33})^2} + \left(c_{11}^s - \frac{d_{31}^s d_{31} \kappa}{1 + \kappa a_{33}} \right) \frac{h^2}{2} \quad (30a)$$

$$D_{12} = \left(c_{12} - \frac{d_{31}^2 \kappa}{1 + \kappa a_{33}} \right) \frac{h^3}{12} - \frac{f_{31}^2 h}{a_{33} (1 + \kappa a_{33})} - \frac{f_{31}^2 h^2}{2\lambda b_{33}} * \frac{e^{\frac{h}{2}\lambda} + e^{-\frac{h}{2}\lambda}}{e^{\frac{h}{2}\lambda} - e^{-\frac{h}{2}\lambda}} + \frac{b_{33} d_{31}^2 \kappa^2 h}{(1 + \kappa a_{33})^2} + \left(c_{12}^s - \frac{d_{31}^s d_{31} \kappa}{1 + \kappa a_{33}} \right) \frac{h^2}{2} \quad (30b)$$

$$D_{66} = \frac{c_{66}}{12} h^3 + \frac{c_{66}^s}{2} h^2 \quad (30c)$$

4. Solution procedure

In this section, a Galerkin solution of the governing equation system is presented for simply-supported (S) and clamped (C) edge conditions

$$w = \frac{\partial^2 w}{\partial x^2} = 0 \quad \text{at } x=0, a$$

$$w = \frac{\partial^2 w}{\partial y^2} = 0 \quad \text{at } y=0, b \quad (31)$$

- Clamped (C):

$$w = \frac{\partial w}{\partial x} = \frac{\partial w}{\partial y} = 0 \quad \text{at } x=0, a \text{ and } y=0, b \quad (32)$$

The double-layered nanoplates experience three kinds of vibrations as indicated in Fig. 2:

- Out of phase vibration: $w = w_1 - w_2 \neq 0$
- In-phase vibration: $w = w_1 - w_2 = 0$
- One nanoplate fixed: $w = w_1 = 0$

First, the transverse displacement with the functions N_i and N_j that satisfy the considered boundary conditions is assumed as

$$w = \sum_{i=1}^{\infty} \sum_{j=1}^{\infty} \tilde{W} N_i(x) N_j(y) e^{i\omega t} \quad (33)$$

where \tilde{W} is the unknown coefficient. Inserting Eq. (33) into the governing equation leads to

$$\left\{ [K]_{i \times j} + \omega^2 [M]_{i \times j} \right\} \left\{ \tilde{W} \right\} = 0 \quad (34)$$

where

$$K = D_{11} (\Lambda_{4000} + \Lambda_{0400}) + 2(D_{12} + 2D_{66}) \Lambda_{2200} + \left(\frac{d_{31}}{a_{33}} V + \frac{2d_{31}^2}{a_{33} h} V - 2\sigma_0 \right) (\Lambda_{2000} + \Lambda_{0200}) + k_0 \lambda \Lambda_{0000} \quad (35)$$

$$M = -\rho \frac{h^3}{12} (\Lambda_{2000} + \Lambda_{0200}) + \rho h \Lambda_{0000} \quad (36)$$

in which λ is equal to 0, 1 or 2 depending on the type of vibration and

$$\Lambda_{0000} = \int_0^a \int_0^b N_i N_j N_i N_j dx dy$$

$$\Lambda_{2000} = \int_0^a \int_0^b N_i'' N_j N_i N_j dx dy$$

$$\Lambda_{0200} = \int_0^a \int_0^b N_i N_j'' N_i N_j dx dy$$

$$\Lambda_{4000} = \int_0^a \int_0^b N_i'''' N_j N_i N_j dx dy$$

$$\Lambda_{0400} = \int_0^a \int_0^b N_i N_j'''' N_i N_j dx dy$$

Here, approximate functions to satisfy the above-mentioned boundary conditions are assumed as

$$\text{SSSS: } N_i(x) = \sin\left(\frac{i\pi}{a}x\right), N_j(y) = \sin\left(\frac{j\pi}{b}y\right) \quad (37)$$

$$\text{CCCC: } N_i(x) = \sin^2\left(\frac{i\pi}{a}x\right), N_j(y) = \sin^2\left(\frac{j\pi}{b}y\right) \quad (38)$$

Also, for better presentation of the results the following dimensionless quantity is adopted

$$\bar{\omega} = \frac{\omega}{\omega_0}, K_0 = k_0 \frac{a^4}{D_{11}}, K_p = k_p \frac{a^2}{D}, \quad (39)$$

where ω_0 is the vibration frequency without surface and flexoelectric effects.

5. Numerical results and discussions

In this section, frequency analysis of a double-layered piezoelectric nanoplate under closed circuit condition will be conducted considering flexoelectric and surface effects.

The top surface of the nanoplate is subjected to an electric voltage, while the bottom surface has no voltage. The flexoelectric nanoplate is made of BaTiO₃ where the elastic properties are considered as $c_{11}=167.55$ GPa, $c_{12}=78.15$ GPa, $c_{66}=44.7$ GPa and the piezoelectric and dielectric coefficients are assumed as $d_{31}=3.5 \times 10^8$ V/m, $a_{33}=0.79 \times 10^8$ Vm/C and $b_{33}=1 \times 10^{-9}$ Jm³/C². The flexoelectric coefficient is also considered as $f_{31}=1-10$ V. The surface elastic and piezoelectric constants for BaTiO₃ can be considered as: $c_{11}^s=9.72$ Pa, $c_{12}^s=4.35$ Pa, $c_{66}^s=2.68$ Pa and $d_{31}^s=-0.056$ C/m.

A verification study of vibration frequencies has been carried out with those of Yang *et al.* (2015) for a single-layer flexoelectric nanoplate under open circuit electric condition. This comparison study is shown in Fig. 3 for a variety of nanoplate thickness and a good agreement is observed. In this figure, only fully simply-supported boundary condition is considered, since there is no published study on vibration behavior of flexoelectric nanoplates with fully clamped edge conditions.

Fig. 4 illustrates the variation of the normalized vibration frequency of flexoelectric nanoplates versus the thickness value for different applied electrical voltages at $a=b=50h$, $f_{31}=10$ and $K_0=100$. In this figure, out-of-phase vibration of system is considered. One can see from this figure that the combined influences of the flexoelectricity and surface on the vibration frequency are dependent on the applied electric voltage. In fact, frequency ratio decreases with the increase of applied voltage from negative to positive values. However, frequency ratio of flexoelectric nanoplate increases with the increment in the thickness value. But, frequency ratio is less affected by the higher values of nanoplate thickness. It means that flexoelectricity effect is more important at smaller values of nanoplate thickness. This feature shows the inherent size-dependent

phenomenon in piezoelectric nanostructures provided by flexoelectricity. The discrepancy of the curves in this figure proposes a possible way for frequency tuning by means of the applied electric voltage. However, such a frequency tuning process in the design of piezoelectric nanostructures may be altered by the combined effects of the flexoelectricity and the surface.

Fig. 5 shows the variation of frequency ratio versus the thickness value for various flexoelectric coefficients when $a=b=50h$, $V=+0.1$ and $K_0=100$ for out-of-phase vibration. In the case without flexoelectricity, only surface effects are considered. It can be seen that increase of flexoelectric coefficient yields smaller frequency ratios. However, the frequency ratio increases with higher rates with respect to nanoplate thickness at higher flexoelectric coefficients. It means that the dependency of vibration behavior of piezoelectric nanoplates on thickness values increases with the rise of flexoelectric coefficient. Such important observation cannot be found in conventional piezoelectric materials. Actually, it is observed from the figure that when no flexoelectricity is considered, the normalized natural frequency is decreasing as the plate size is increasing.

For a square nanoplate ($a = b = 50h$) subjected to a voltage ($V=+0.1$), the variation of the normalized frequency with the plate thickness h is depicted in Fig. 6 for both SSSS and CCCC boundary conditions. It can be deduced that with the considered surface material parameters and the flexocoupling coefficients, both the surface effects and the flexoelectricity influence the vibration frequency significantly. Actually, the surface effects may enhance the frequency ratio with a positive residual surface stress but reduce the resonant frequency with a negative one. Because of the opposite trends of the flexoelectricity and the positive residual surface stress upon the frequency ratio, the size-dependent vibration may disappear. However, the combined effects are more pronounced for the thinner plates with smaller thickness and diminish with the increasing plate thickness as indicated by all the curves tending to approach a unity. Thus, it is necessary to incorporate both the flexoelectricity and surface effects in investigating the dynamic response of nanoscale piezoelectric structures.

Fig. 7 indicates the variation of frequency ratio versus interlayer stiffness (K_0) for various types of vibration when $a=b=50h$, $V=+0.1$ and $f_{31}=5$. It is found that presence of interlayer elastic medium has a significant effect on the vibration behavior of flexoelectric nanoplates. As stated, in-phase vibration of system is not affected by the interlayer stiffness. In two other cases interlayer elastic medium makes the flexoelectric nanoplate system more rigid and vibration frequencies increase. However, out-of-phase frequency ratio is more influenced by the interlayer elastic medium compared with when one nanoplate is fixed. Also, a SSSS flexoelectric nanoplate system is more affected by the interlayer elastic medium, since clamped edges make the nanoplate more rigid. Then, effect of interlayer elastic medium on frequency ratio of a nanoplate system with CCCC edges is less significant than those with SSSS edge conditions.

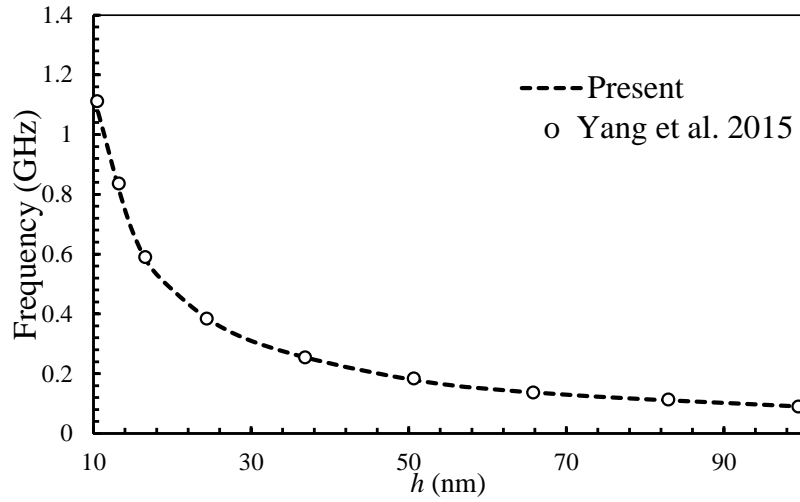


Fig. 3 Comparison of natural frequency of flexoelectric nanoplates ($a=b=50h$)

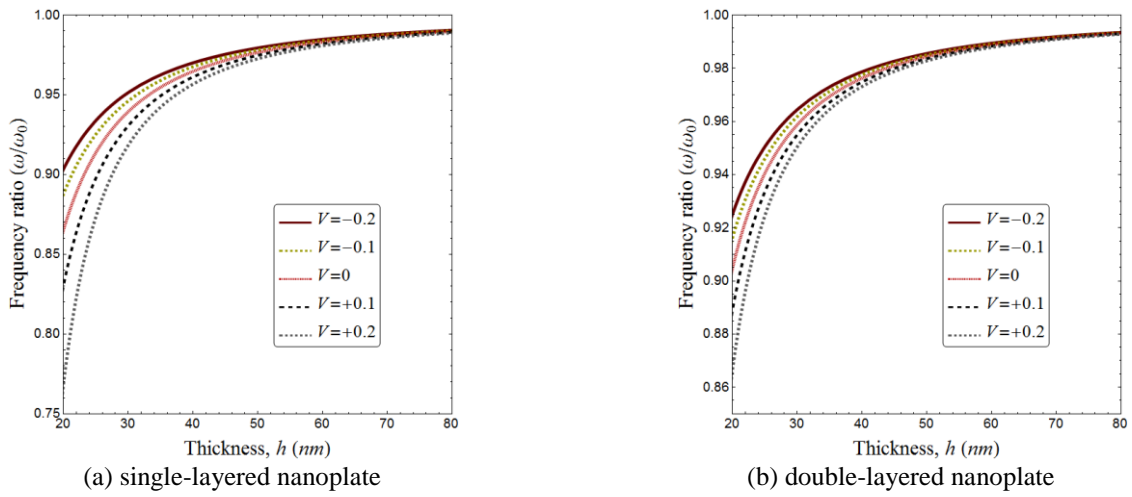


Fig. 4 Variation of frequency ratio versus the thickness value for different applied electric voltages ($a=b=50h, f_{31}=10, K_0=100$)

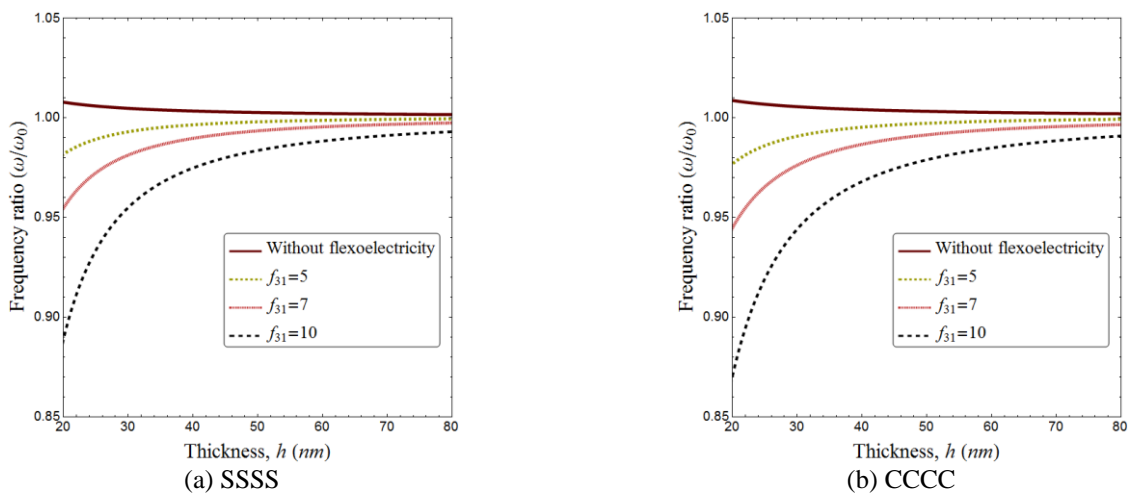


Fig. 5 Variation of frequency ratio versus the thickness value for various flexoelectric coefficients ($a=b=50h, V=+0.1, K_0=100$)

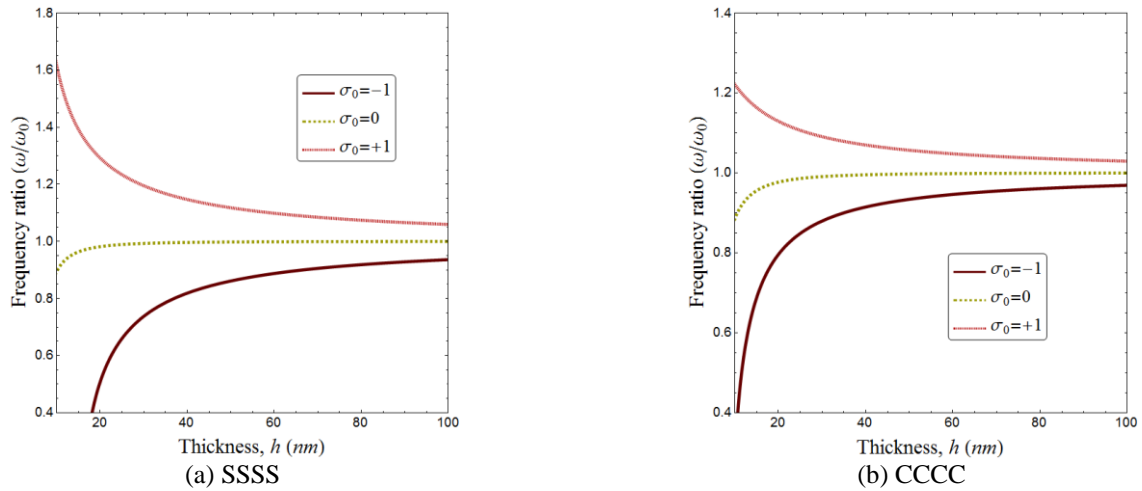


Fig. 6 Variation of frequency ratio versus the thickness value for various values of residual surface stress ($a=b=50h$, $V=+0.1$, $f_{3I}=5$, $K_0=100$)

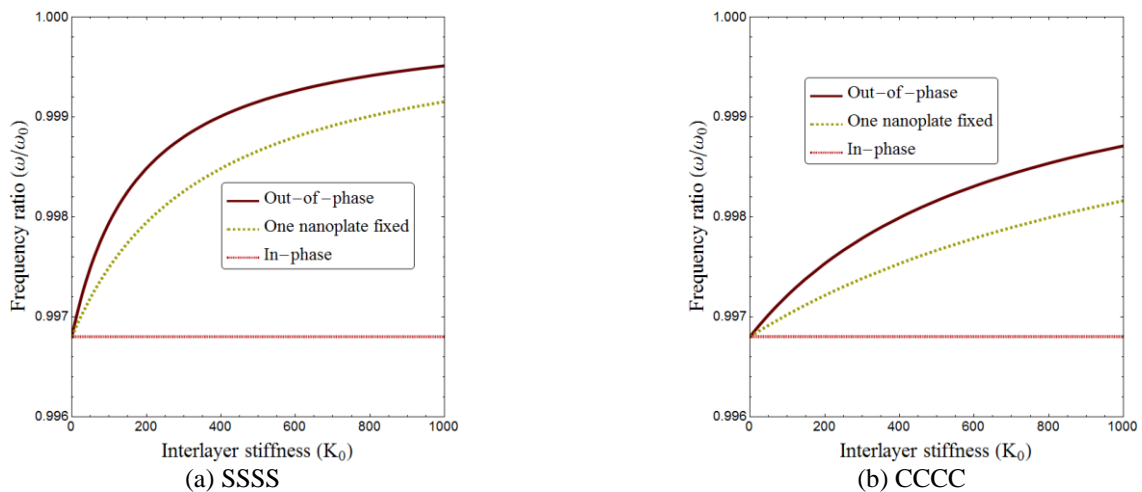


Fig. 7 Variation of frequency ratio versus interlayer stiffness for various types of vibration ($a=b=50h$, $V=+0.1$, $f_{3I}=5$)

6. Conclusions

This paper develops a size-dependent and double-layered flexoelectric nanoplate system incorporating surface effects for vibration analysis of elastically bonded piezoelectric nanoplates. The governing differential equation and related boundary edges were derived by exploiting the use of the Hamilton's principle. The governing equation solution is provided employing Galerkin's approach which has the potential to capture various boundary conditions. It is found that with increase of nanoplate thickness the strain gradients reduce and flexoelectricity can be negligible. Actually, flexoelectricity is more important at smaller thickness. However, vibration frequencies depend on the sign and values applied electric voltage and residual surface stress. Also, interlayer elastic medium has a great influence on vibration behavior of double-layered flexoelectric nanoplates depending on the type of vibration.

References

- Ahouel, M., Houari, M.S.A., Bedia, E.A and Tounsi, A (2016), "Size-dependent mechanical behavior of functionally graded trigonometric shear deformable nanobeams including neutral surface position concept", *Steel Compos. Struct.*, **20**(5), 963-981.
- Akbas, S.D. (2016), "Forced vibration analysis of viscoelastic nanobeams embedded in an elastic medium", *Smart Struct. Syst.*, **18**(6), 1125-1143.
- Arani, A.G., Kolahchi, R. and Zarei, M.S. (2015), "Visco-surface-nonlocal piezoelectricity effects on nonlinear dynamic stability of graphene sheets integrated with ZnO sensors and actuators using refined zigzag theory", *Compos. Struct.*, **132**, 506-526.
- Asemi, S.R., Farajpour, A. and Mohammadi, M. (2014), "Nonlinear vibration analysis of piezoelectric nanoelectromechanical resonators based on nonlocal elasticity theory", *Compos. Struct.*, **116**, 703-712.
- Asemi, S.R., Farajpour, A., Asemi, H.R. and Mohammadi, M. (2014), "Influence of initial stress on the vibration of double-piezoelectric-nanoplate systems with various boundary conditions using DQM", *Physica E: Low-dimensional Syst.*

- Nanostruct.*, **63**, 169-179.
- Barati, M.R. and Shahverdi, H. (2017), "Small-scale effects on the dynamic response of inhomogeneous nanobeams on elastic substrate under uniform dynamic load", *The European Physical Journal Plus*, **132**(4), 167.
- Bounouara, F., Benrahou, K.H., Belkorissat, I. and Tounsi, A. (2016), "A nonlocal zeroth-order shear deformation theory for free vibration of functionally graded nanoscale plates resting on elastic foundation", *Steel Compos. Struct.*, **20**(2), 227-249.
- Ebrahimi, F. and Barati, M.R. (2016), "A nonlocal higher-order refined magneto-electro-viscoelastic beam model for dynamic analysis of smart nanostructures", *Int. J. Eng. Sci.*, **107**, 183-196.
- Ebrahimi, F. and Barati, M.R. (2017a), "Damping vibration analysis of smart piezoelectric polymeric nanoplates on viscoelastic substrate based on nonlocal strain gradient theory", *Smart Mater. Struct.*, **26**(6), 065018.
- Ebrahimi, F. and Barati, M.R. (2017b), "Surface effects on the vibration behavior of flexoelectric nanobeams based on nonlocal elasticity theory", *The European Physical Journal Plus*, **132**(1), 19.
- Ebrahimi, F. and Barati, M.R. (2017c), "Vibration analysis of size-dependent flexoelectric nanoplates incorporating surface and thermal effects", *Mech. Adv. Mater. Struct.*, 1-11.
- Ebrahimi, F. and Salari, E. (2017), "Semi-analytical vibration analysis of functionally graded size-dependent nanobeams with various boundary conditions", *Smart Struct. Syst.*, **19**(3), 243-257.
- Elmerabet, A.H., Heireche, H., Tounsi, A. and Semmah, A. (2017), "Buckling temperature of a single-walled boron nitride nanotubes using a novel nonlocal beam model", *Adv. Nano Res.*, **5**(1), 1-12.
- Eringen, A.C. (1983), "On differential equations of nonlocal elasticity and solutions of screw dislocation and surface waves", *J. Appl. Phys.*, **54**(9), 4703-4710.
- Gholami, R. and Ansari, R. (2017), "A unified nonlocal nonlinear higher-order shear deformable plate model for postbuckling analysis of piezoelectric-piezomagnetic rectangular nanoplates with various edge supports", *Compos. Struct.*, **166**, 202-218.
- Gurtin, M.E. and Ian Murdoch, A. (1975), "A continuum theory of elastic material surfaces", *Arch. Ration. Mech. An.*, **57**(4), 291-323.
- Karimi, M. and Shahidi, A.R. (2017), "Nonlocal, refined plate, and surface effects theories used to analyze free vibration of magneto-electroelastic nanoplates under thermo-mechanical and shear loadings", *Appl. Phys. A*, **123**(5), 304.
- Li, L. and Hu, Y. (2016), "Nonlinear bending and free vibration analyses of nonlocal strain gradient beams made of functionally graded material", *Int. J. Eng. Sci.*, **107**, 77-97.
- Li, L., Li, X. and Hu, Y. (2016), "Free vibration analysis of nonlocal strain gradient beams made of functionally graded material", *Int. J. Eng. Sci.*, **102**, 77-92.
- Li, Y.S. and Pan, E. (2016), "Bending of a sinusoidal piezoelectric nanoplate with surface effect", *Compos. Struct.*, **136**, 45-55.
- Liang, X., Hu, S. and Shen, S. (2014), "Effects of surface and flexoelectricity on a piezoelectric nanobeam", *Smart Mater. Struct.*, **23**(3), 035020.
- Liang, X., Yang, W., Hu, S. and Shen, S. (2016), "Buckling and vibration of flexoelectric nanofilms subjected to mechanical loads", *J. Phys. D: Appl. Phys.*, **49**(11), 115307.
- Ray, M.C. (2016), "Analysis of smart nanobeams integrated with a flexoelectric nano actuator layer", *Smart Mater. Struct.*, **25**(5), 055011.
- Shen, J.P., Li, C., Fan, X.L. and Jung, C.M. (2017), "Dynamics of silicon nanobeams with axial motion subjected to transverse and longitudinal loads considering nonlocal and surface effects", *Smart Struct. Syst.*, **19**(1), 105-113.
- Wang, W., Li, P., Jin, F. and Wang, J. (2016), "Vibration analysis of piezoelectric ceramic circular nanoplates considering surface and nonlocal effects", *Compos. Struct.*, **140**, 758-775.
- Yan, Z. (2016), "Size-dependent bending and vibration behaviors of piezoelectric circular nanoplates", *Smart Mater. Struct.*, **25**(3), 035017.
- Yan, Z. and Jiang, L. (2013), "Size-dependent bending and vibration behaviour of piezoelectric nanobeams due to flexoelectricity", *J. Phys. D: Appl. Phys.*, **46**(35), 355502.
- Yang, W., Liang, X. and Shen, S. (2015), "Electromechanical responses of piezoelectric nanoplates with flexoelectricity", *Acta Mechanica*, **226**(9), 3097-3110.
- Zang, J., Fang, B., Zhang, Y.W., Yang, T.Z. and Li, D.H. (2014), "Longitudinal wave propagation in a piezoelectric nanoplate considering surface effects and nonlocal elasticity theory", *Physica E: Low-dimensional Syst. Nanostruct.*, **63**, 147-150.
- Zhang, L.L., Liu, J.X., Fang, X.Q. and Nie, G.Q. (2014), "Effects of surface piezoelectricity and nonlocal scale on wave propagation in piezoelectric nanoplates", *Eur. J. Mech.-A-Solid*, **46**, 22-29.
- Zhang, Y., Hong, J., Liu, B. and Fang, D. (2009), "Strain effect on ferroelectric behaviors of BaTiO₃ nanowires: a molecular dynamics study", *Nanotechnology*, **21**(1), 015701.
- Zhang, Z. and Jiang, L. (2014), "Size effects on electromechanical coupling fields of a bending piezoelectric nanoplate due to surface effects and flexoelectricity", *J. Appl. Phys.*, **116**(13), 134308.

FC